Vertical seismic profiling and seismic properties of gas hydrate in an Arctic well

Yanpeng Mi[1], Akio Sakai[2], Rakesh Walia[3], Roy D. Hyndman[4], and Scott R. Dallimore[5]

ABSTRACT

Gas hydrate is an ice-like nonstochiometric inclusion compound with water molecules forming a three-dimensional network within which small gas molecules (guest) can be trapped. In a collaborative Japan-Canada research project, a 1150 m research well was drilled in the Canadian Arctic to investigate gas hydrates beneath permafrost. The well located in the Mackenzie Delta, N.W.T. was part of a Japanese government-industry program to assess the potential of gas hydrates as an energy source. The primary objectives of the well were to evaluate drilling, coring and geophysical technologies prior to gas hydrate drilling program offshore Japan. The project involved comprehensive downhole measurements and laboratory studies on recovered cuttings and core. This article reports the results of vertical seismic profiling surveys (VSP), which have been used along with downhole log data, to evaluate the effect of gas hydrate on velocity and to estimate gas hydrate concentrations. VSP was recorded for both vertical and offset source positions, using multi-component receiver tools and multi-polarized vibrators. The excellent data quality allows accurate compressional and shear wave velocity profiling, as well as reliable estimation of the gas hydrate effect on sediment elastic properties. Major reflectors, such as the base of the permafrost zone and the hydrate host strata, were clearly seen in the VSP data. Corridor stack of zero-offset P-wave data and VSP-CDP transform of offset data provide good comparisons with the surface seismic data. Velocities in the permafrost section above 620 m are markedly increased by ice bonding and are generally over 2500 m/s. In the largely unfrozen section from 620 m to 890 m, the velocities are lower, and range from 2000 m/s to 2400 m/s. In the main gas hydrate zone below 890 m to the base of the hydrate stability zone at around 1100 m, velocities are increased by hydrate cementation up to 2500-3700 m/s. The estimated hydrate saturations are highly variable, reaching as high as 60% in short sections, with an average of about 20% (~7% of sediment volume for 35% porosity) in the 900-1100 m interval. Poisson's Ratio is ~0.39 in both the permafrost and gas hydrate sections compared to ~0.44 in the unfrozen sections. The seismic properties indicate that the hydrate is located mainly in the sediment pores, rather than cementing the grain contacts, and that commonly used velocity versus hydrate concentration relations are approximately valid. Gas hydrate stiffen the sediment matrix and should cause less seismic attenuation effect, hence a higher seismic quality factor (Q) than that of normal sediment. The power ratio method gave a Q of about 30 in the dominant bandwidth from 50 Hz to 100 Hz, while higher Q value for higher frequency within the normal sediment. The destructive interbed multiples caused by hydrate layers prevented even a rough Q value estimation.

[1] CREWES Project, Dept. Geology and Geophysics, University of Calgary, Calgary, Alberta, [2] Japan Petroleum Exploration Co., Ltd. (JAPEX), Tokyo, Japan, [3] CGG Canada, Calgary, Alberta, [4] Pacific Geoscience Center, Geological Survey of Canada, Sidney, B.C., [5] Terrain Sciences Division, Geological Survey of Canada, Ottawa,

INTRODUCTION

Natural gas hydrate has received intensive recent study because of its potential as a future energy resource and its possible role in climate change. Gas hydrate has been inferred to occur in large areas beneath continental slopes at temperate latitudes, and beneath permafrost in arctic land and continental shelf regions, where the conditions for natural gas hydrate formation and stability occur. Natural gas hydrate was first clearly recognized in the western Canadian Arctic in the early 1970s where it resulted in the blowout of a Mackenzie Delta exploration well (Bily and Dick, 1974). Subsequently gas hydrate has been recognized to be widespread in Arctic Canada and Alaska both beneath land and shallow continental shelf areas (Judge et al. 1988, Dallimore and collet, 1995). In the Mackenzie Delta (**Figure 1**), gas hydrate has been identified in approximately 17% of exploration wells (Dallimore et al., 1998). However, little is known as yet about the geological controls of hydrate formation, preservation and thus distribution (e.g., Dallimore et al., 1998).

A research well JAPEX/JNOC/GSC Mallik 2L-38 was drilled in the Canadian Arctic in 1998 to investigate gas hydrates beneath permafrost, in a collaborative research project between the Japan National Oil Corporation (JNOC) and the Geological Survey of Canada (GSC). Other principal participants in the project included Japan Petroleum Exploration Company Limited (JAPEX), and the U.S. Geological Survey (USGS), along with a number of other Japanese and North American institutes and companies. The 1150 m deep research well is located in the Mackenzie Delta, N.W.T., Canada at 69^o 27.7' N; 134^o 39.5' W; elevation 1.1 m (figure 1). The site is located close to the Mallik L-38 well which was drilled by Imperial Oil in 1972. L-38 and previous seismic lines showed clear evidence of gas hydrate (figure 2). The new well was part of a Japanese government-industry program to assess the potential of gas hydrate as an energy source. It was intended to evaluate drilling, coring and geophysical technologies prior to offshore gas hydrate research drilling planned for off southwest Japan by JNOC. The overall objectives, program management and operations are described by Dallimore et al. (1998; 1999). The multidisciplinary borehole study included permafrost and gas hydrate coring, comprehensive downhole geophysical logging and measurements, and laboratory measurements on recovered cuttings and cores. The laboratory studies included sedimentology, physical properties, geochemistry and reservoir characteristics of the formation.

As part of the Mallik 2L-38 field program, a VSP survey was carried out at vertical and offset source positions, using multi-component receiver tools and multi-polarized vibrator sources. The survey was carried out by Schlumberger Ltd. in March 1998, with field operation planning and direction by A. Sakai of JAPEX (Sakai, 1998; 1999). A special effort was made to record high quality shear wave data, as well as compressional wave data. Results from this work will be integrated with down hole logs and regional seismic data. The data will also be used to determine the effect of gas hydrate on formation velocities and to estimate gas hydrate concentrations as a function of depth in the formation penetrated by the well. Initial reports on the VSP data and analyses have been given by Sakai (1999) and Walia et al. (1999). This report gives a more complete description of the processing, results and interpretation of the VSP data.

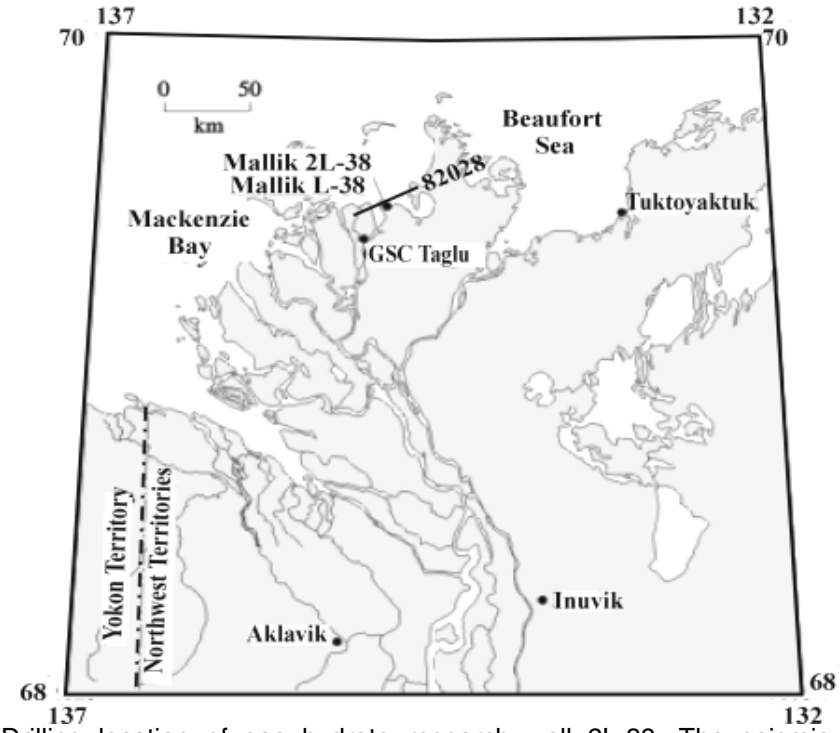

Figure 1. Drilling location of gas hydrate research well 2L-38. The seismic line 82028 acquired by Imperial Oil Limited in 1982 is also shown.

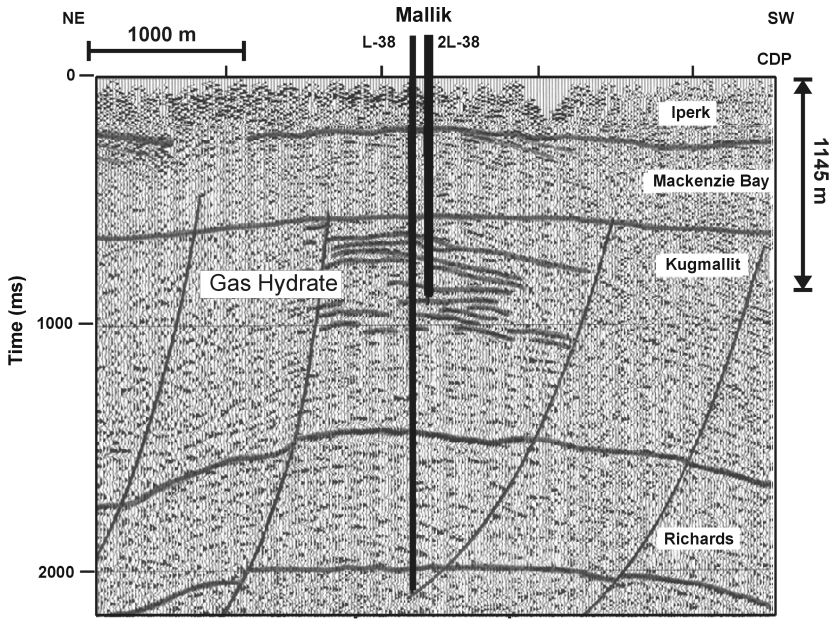

Figure 2. Previous surface seismic data indicates gas hydrate presence in the vicinity of well L-38 and 2L-38 (after Dallimore, 1999).

GEOLOGICAL SETTING AND SEDIMENT SECTION

The Beaufort-Mackenzie Cretaceous-Holocene sediment section lies over the highly faulted Lower Cretaceous structural basement. Based on reflection seismic profiling, well log data and limited outcrop information, Dixon and Dietrich (1988) and Dixon et al. (1992) subdivided the early Cretaceous to Holocene sediment section into eleven regionally extensive, transgression-regression sequences (figure 3). The research well penetrated the upper Oligocene to Holocene sediments which consist of three of the sequences. From the top to the bottom of the well, they are, (1) Iperk sequence (0-346 m), which is mainly composed of ice-bounded sand with occasional conglomerate silt and clay layers; (2) Mackenzie Bay sequence (346-926.5 m), which is mainly composed of sand and weakly cemented sandstone with silt/shale interbeds; and (3) Kugmallit sequence (below 926.5 m), mainly composed of weakly cemented sandstone and siltstone (Jenner, 1998). The base of the ice-bonded permafrost zone occurs at about 640 m. In the well the main gas hydrate occurrences is in a 113 m thick sequence of gas hydrate bearing sand and silty clay between 897 m to 1110 m.

Gas hydrate pressure-temperature stability conditions extend from a depth of about 180 m to near the bottom of the well (Dallimore, 1998). Hydrate however is found mainly in the 200 m interval above the base of the stability zone. Adequate methane for significant hydrate production appears to be limited to this lower part of the stability zone. That hydrate is concentrated in the lower portion of stability zones has been recognized in a number of deep sea occurrences (Hyndman and Spence, 1992; Andreassen, 1995; Yuan et al., 1996). On a finer scale, the occurrence of gas hydrate seems strongly controlled by lithology. For the most part, the gas hydrate occurs within coarse-grained sandy sediments. The sandy sequences are typically interbedded with non-hydrate bearing fine-grained clays and silts. There also appears to be a correlation between hydrate occurrence and oil and gas occurrence. Among the eleven sedimentary sequences identified by Dixon (1992), oil or gas have been found in five (figure 3).

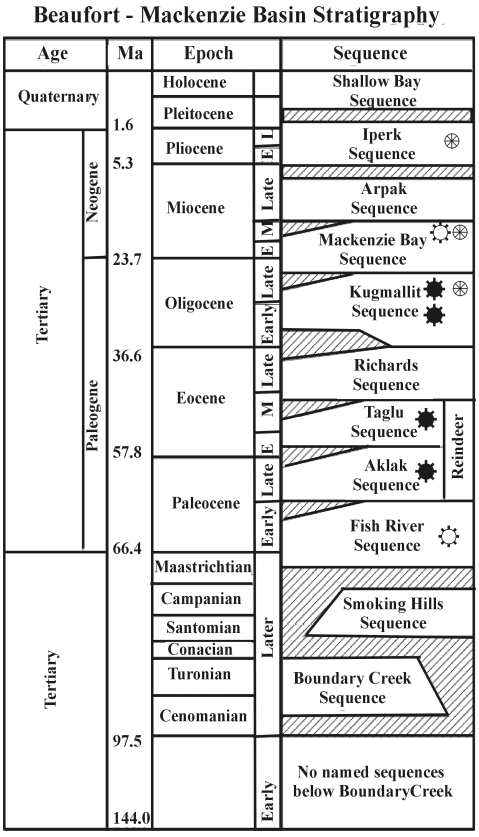

Figure 3. Sediment stratigraphy from early Creataceous to Holocene of the Beaufort-Mackenzie area (after Dixon, 1992). Closed circles, open circles and circles with a cross indicate the presence of oil, gas and gas hydrate, respectively.

VSP SURVEY AND DATA

The VSP survey included both zero offset, near vertical recording and offset recording, and vertical and horizontal vibrators. Sakai (1998) provided VSP survey parameter details. The two sources were IVI MiniVibrators for compressional and shear modes (transverse to the well). The zero-offset, vertical recording was from 500 to 1145 m, at intervals of 5 m for the compressional source and 15 m for the shear source in transverse mode. For the offset VSP, recording was from 240 to 1145 m and the compressional source was recorded at 5 m intervals. The source signal was a 12 s linear sweep with frequency band 10-200 Hz for the zero-offset compressional source, 10-100 Hz for the offset compressional source and 10-50 Hz for the zero-offset shear source. The shear source was not recorded at the offset position. The listening time was 3 s and the sampling rate was 1 ms. The near zero-offset source was 40 m from the well head. The offset source was 401 m from the well, approximately on the line of a previous surface seismic survey. This offset distance was found to be the maximum for a good signal. Sakai (1998) described the special efforts made to optimize the coupling of the vibrator to the ground and to reduce ambient noise in the permafrost environment. Wind noise significantly influenced data quality, especially for the low frequency shear wave data.

Downhole recording employed two directly connected Schlumberger three-component Combined Seismic Imager (CSI) tools with a 300 Hz low pass filter. The hole was cased above 676 m, and in the upper 250 m the casing contact with the formation was poor and the recorded signals were weak. In the open hole portion, the previously collected downhole logs were used to select the optimal receiver positions and to avoid caved sections. The hole condition was especially good, near gauge in the hydrate cemented zone. Vertical and horizontal vibration data were recorded alternatively. There were nominally five recorded traces for each receiver depth, but more vibrator shots were carried out if the data quality was poor. Several test shots were carried out at irregular receiver depths. They were included in the data reorganisation and sorting, but excluded in further processing, especially in wavefield separation.

VSP DATA PROCESSING, VELOCITY ANALYSIS AND IMAGING

The preliminary VSP processing and analysis included: (1) up and downgoing wavefields separation and corridor stack for zero offset P-wave data, imaging by VSP-CDP transform of offset P-wave data, common receiver stack for shear wave data, correlation analysis between VSP-CDP transform with surface multichannel seismic data, (2) first breaks picking and calculation of P and S velocity-depth profile. Poisson's ratio was derived from the zero-offset VSP velocity profile only, because there was now shear source data acquired for offset VSP, (3) gas hydrate saturation estimation from P-wave velocity profile, using weighted equation method and porosity reduction method, (4) seismic quality factor (Q) estimation for normal sediment and hydrate-host sediment section.

For P and S-wave velocity analysis and subsurface imaging, the primary data are zero-offset vertical vibration Z component (P-wave), zero-offset horizontal vibration X component (S-wave) and offset vertical vibration Z component data. There was

limited energy in the cross-orientations, i.e., vertical source and horizontal receiver, or horizontal source with vertical receiver. These are not included in this preliminary study.

Table 1. VSP survey data

Source Offset	Receiver/Source Orientation	Receiver Depth Interval	Depth Range	Source Frequency Range
Zero (40 m)	X/Vertical and horizontal	Vertical source: 5 m Horizontal source:15m	500 m to 1145 m	Vertical: 10-200 Hz Horizontal:10-50 Hz
	Y/Vertical and horizontal			
	Z/Vertical and horizontal			
Offset (400.7m)	X/Vertical vibration	5 m	240 m to 1145 m	Vertical:10-100 Hz
	Y/Vertical vibration			
	Z/Vertical vibration			

VELOCITY ANALYSES

VSP provides more accurate average velocities than the downhole sonic log, but with much poorer depth resolution. First arrivals were picked for the zero-offset vertical vibration Z-component data (P-wave), horizontal vibration X-component data (S-wave) and offset Z-component data (P-wave). Interval P and S-wave velocities were then calculated. For higher resolution in first arrival picking, the vertical vibration Z-component data were resampled to 125 *us* from the recorded 1 *ms* sample rate. The horizontal vibration X-component data were resampled to 250 *us* sample rate.

A wavelet processing sequence was applied to P-wave components and is listed in Table 2. For offset P-wave data, VSP-CDP transform was used to image the subsurface in the vicinity of the well. The zero-offset shear wave data has rather low frequency, overlapping with the strong wind noise from the rig. There was hardly any coherent signal after the first break and efforts made to separate the downgoing and upgoing wavefields turned out to be in vain. Figure 4 shows the main processing results.

Major reflection events show up in both the zero-offset and offset P-wave data. The basement of the permafrost zone at about 600 m (0.33 s TWT) and the three major gas hydrate cemented sediment layers at about 900 m (0.65 s TWT), 980 m (0.70 s TWT) and 1080 m (0.80 s TWT), are quite clear in both the aligned upgoing zero-offset P section and the VSP-CDP transformed offset P section. These events correlates with the high velocity zones in both the sonic log data and the velocity profile derived from VSP data. Gas hydrate layers are roughly horizontal and continuous in the vicinity of the well.

P-wave VSP data provided a more reliable velocity estimation across the gas hydrate zone. P-wave velocity profiles derived from the zero offset and offset P-wave data has excellent correlation, which suggests that the strata near the well are nearly horizontal and that there is no strong anisotropic effect (figure 5). The velocity error introduced by the first break picking should be less than 5% for P-wave velocities.

Compared to the P-wave velocity, shear wave velocities from the VSP are less reliable because of the uncertainty in first break picking. Excessively high shear velocity at 950 m does seem to be true.

The P velocity profile correlates well with the sonic log. P-wave velocities within the gas hydrate zone, from 890m to the bottom of the well, are generally 100-1000 m/s higher than that in the non-hydrate sediments, but generally lower than those in the permafrost zone above 620 m.

Table 2. Wavelet processing flow

Processing steps	Description
1	Trace editing;
2	Geometrical spreading correction: time power 1.0
3	3-loop trim statics application
4	Ensemble amplitude balancing
5	Stacking at constant recording depth, resampling and first break picking
6	F-X noise reduction
7	F-K domain wavefield separation
8	Wavelet extraction, inverse filter calculation and application on up-going wavefield
9	Corridor stack of up-going wavefield

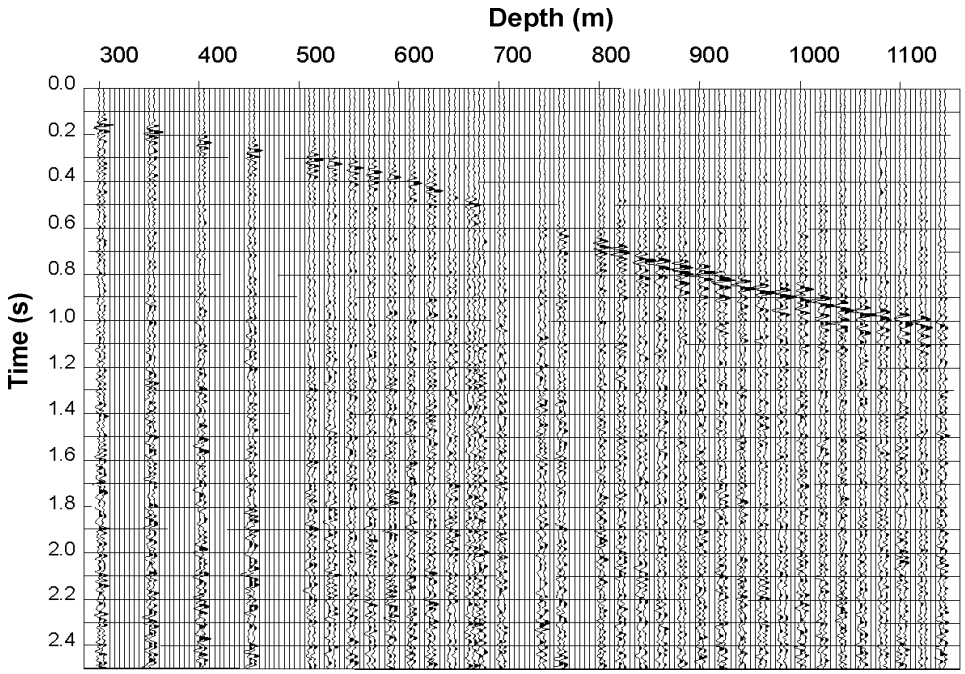

(a) Full wavefield of Zero-offset horizontal vibration X component. Dummy traces were inserted at missing levels. Hardly any events occur after the first break.

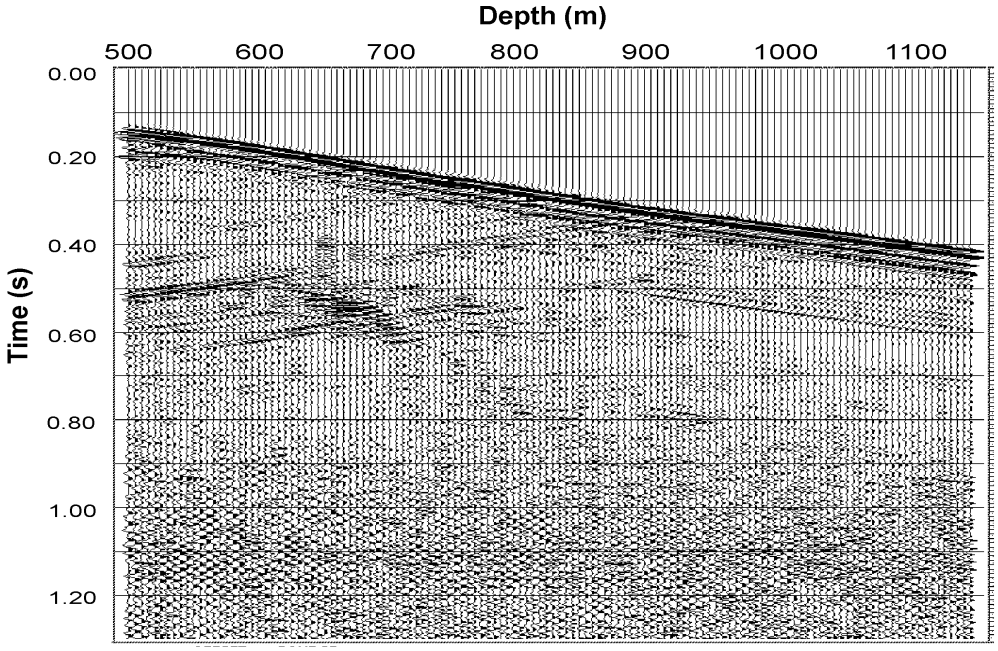

(b) Full wavefield of zero-offset vertical vibration Z component.

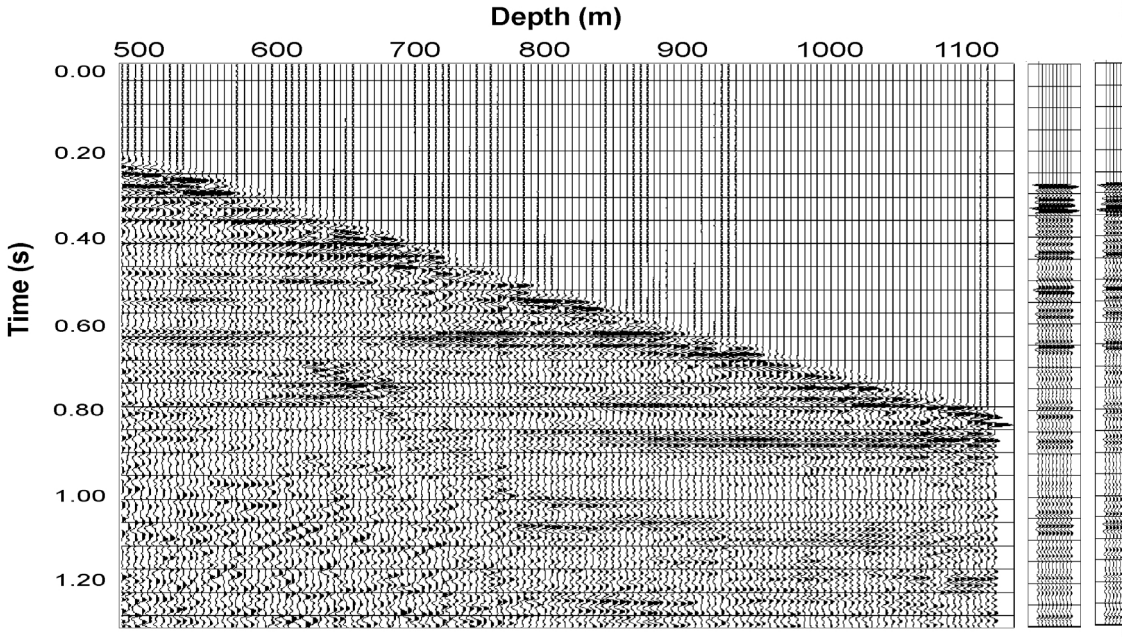

(b) Upgoing wavefield and corridor stack results in normal and reverse polarity.

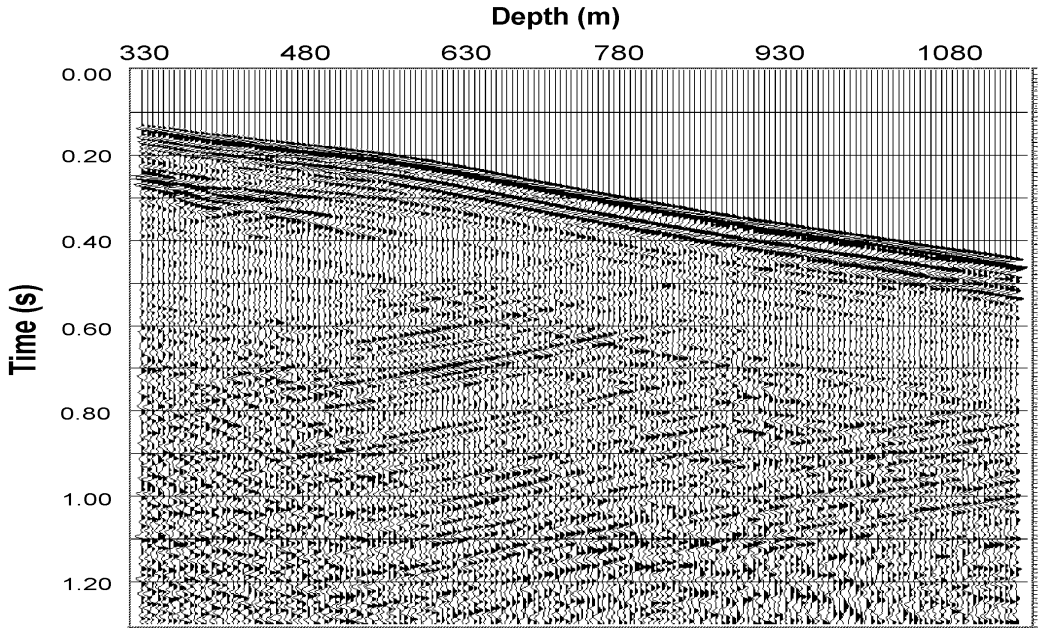

(d) Full wavefield of the offset vertical vibration Z component data.

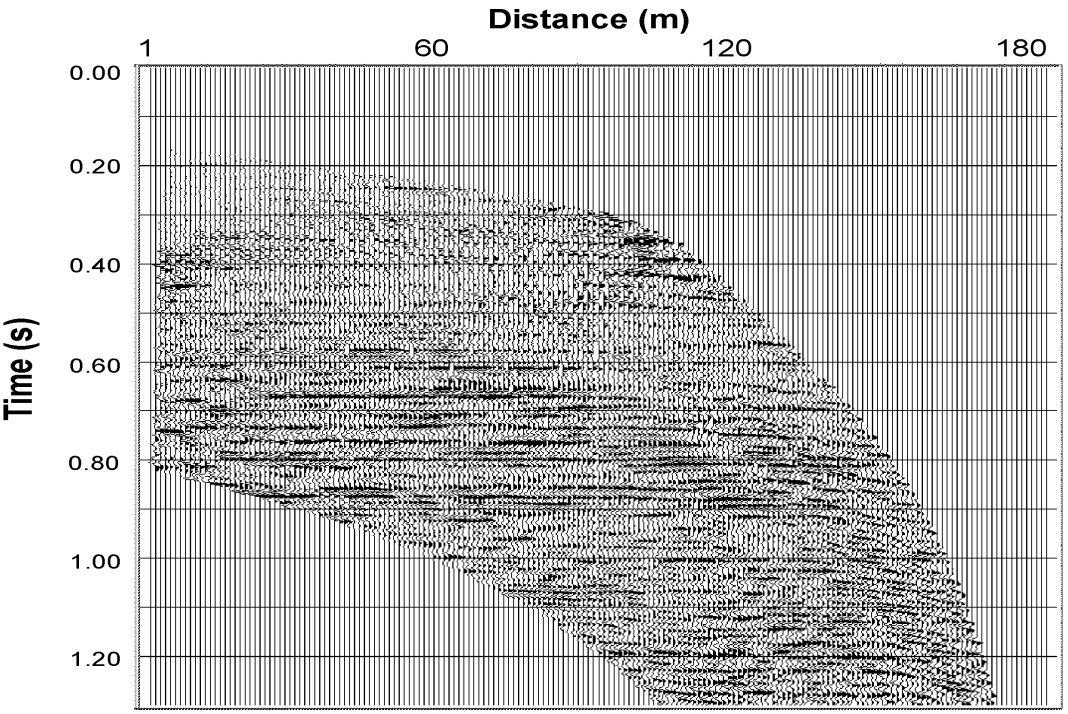

(e) VSP-CDP transform of the upgoing wavefield separated from (d). The surface CDP interval is 1m, covering 0-200 m from the well head in the direction to the source.

Figure 4. Processing results of (a) zero-offset horizontal vibration X component data, (b) and (c) zero-offset vertical vibration Z component data and (d) and (e) offset vertical vibration Z component data.

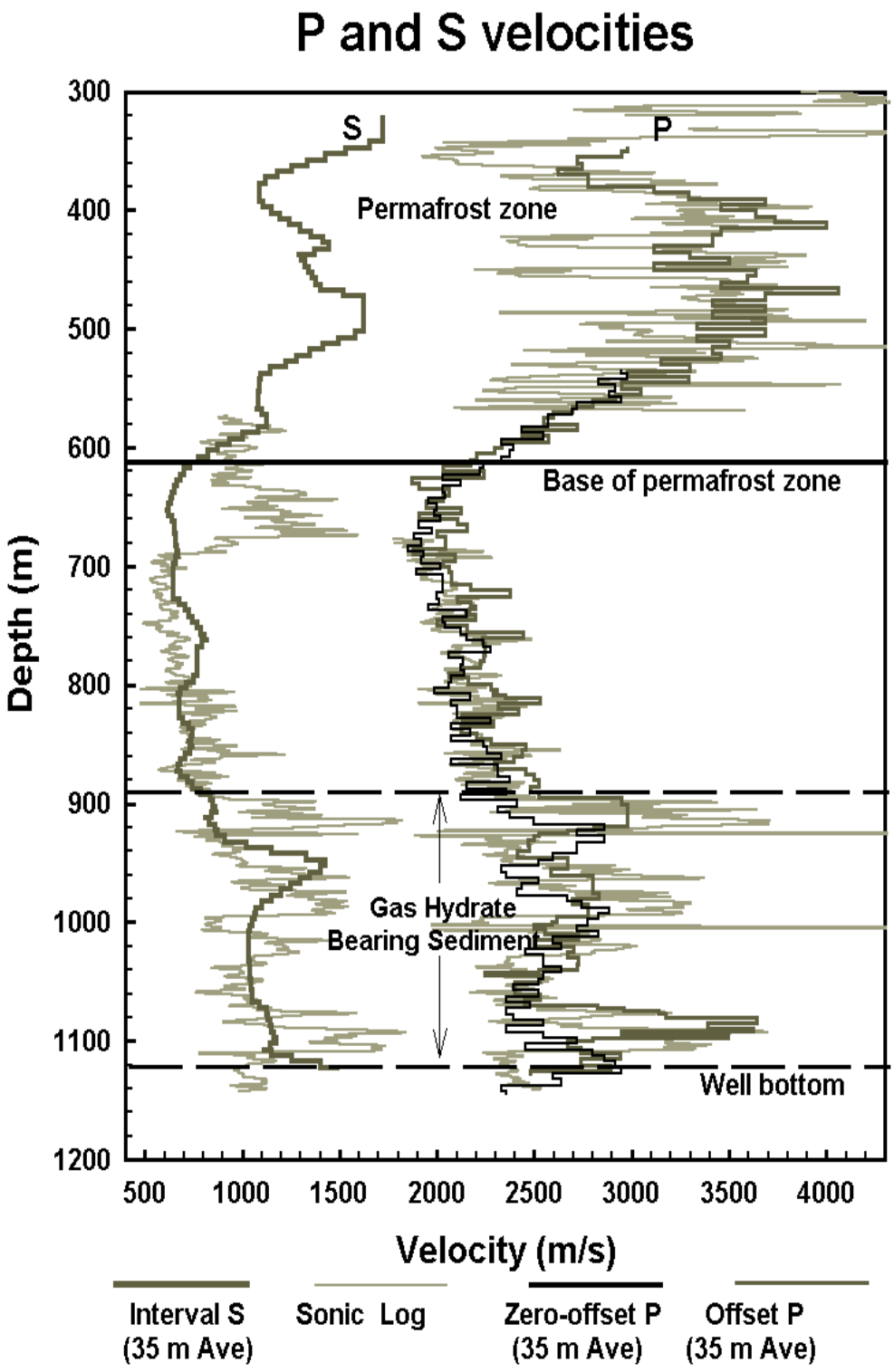

Figure 5. Vp and Vs derived from VSP and sonic log analysis. High Vp from 890 m to the bottom of the hole indicates the presence of gas hydrate.

VP/VS, POISSON'S RATIO AND GENERAL PHYSICAL PROPERTIES

Shear wave velocity of gas hydrate has been calculated using Castagna's Vp-Vs relationship (Castagna, 1985) where only P-wave velocities are available (e.g. Lee et al, 1996; Yuan et al, 1996). However, the velocity logging within the gas hydrate zone presents a different scenario (figure 6). The Vp-Vs relationship derived from the well log is Vp=1.044+1.428Vs, or Vs=-0.731+0.7003Vp. The parameters were calculated in a least-square square sense, with a correlation factor of 0.946. The shear wave velocity predicted from Castagna's formula is generally higher than the measured above the 2400-2500 m/s reference velocity. One possible explanation for this phenomena is that Castagna's formula is for clastic rocks, which should have a higher matrix shear wave velocity than the semi-consolidated gas hydrate host sediment.

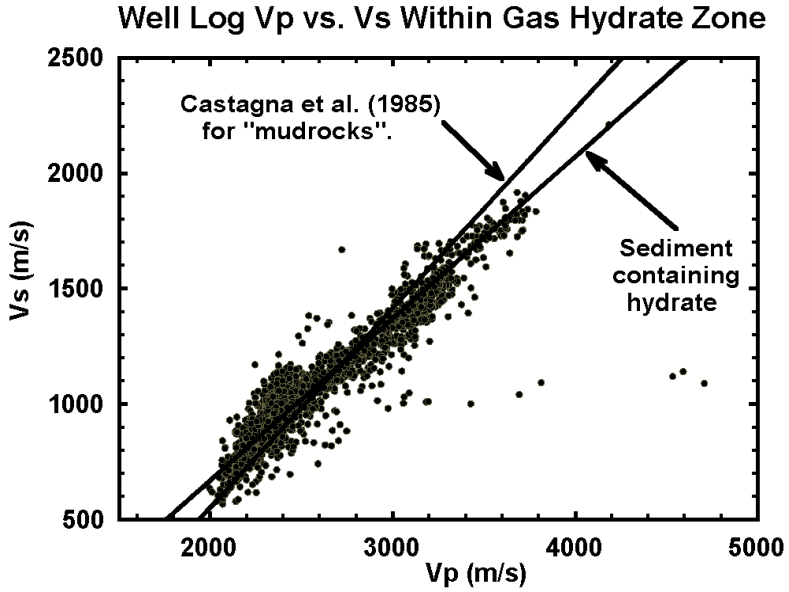

Figure 6. Vp-Vs relationship from sonic log within the gas hydrate zone. The optimum linear fit, Vp=1.044+1.428Vs, or Vs=-0.731+0.7003Vp is slightly different from that derived by Castagna (1985).

Poisson's ratio of pure gas hydrate is about 0.33, as measured in the laboratory (Whalley, 1980; Pandit and King, 1983). However, no direct measurement on Poisson's ratio of partially hydrate-cemented sediment has ever been done. Yuan et al. (1999) conclude that AVO analysis using Poisson's ratio contrast experiences difficulties in discriminating the interface between hydrate-filled sediment/normal sediment and the interface between normal sediment and free-gas-bearing sediment, since both cases lead to a mild decrease in Poisson's ratio. Figure 7a shows the Poisson's ratio and Vp/Vs variation for the normal sediment (620-890 m) and the gas hydrate host sediment (890-1150 m). Poisson's Ratio is generally higher in the normal sediment (0.41-0.45) than in the hydrate host sediment (0.31-0.42), while both show a decreasing trend, as a result of increased shear wave velocity due to normal compaction and hydrate cementation. Density and porosity from the well log are shown in figure 7b.

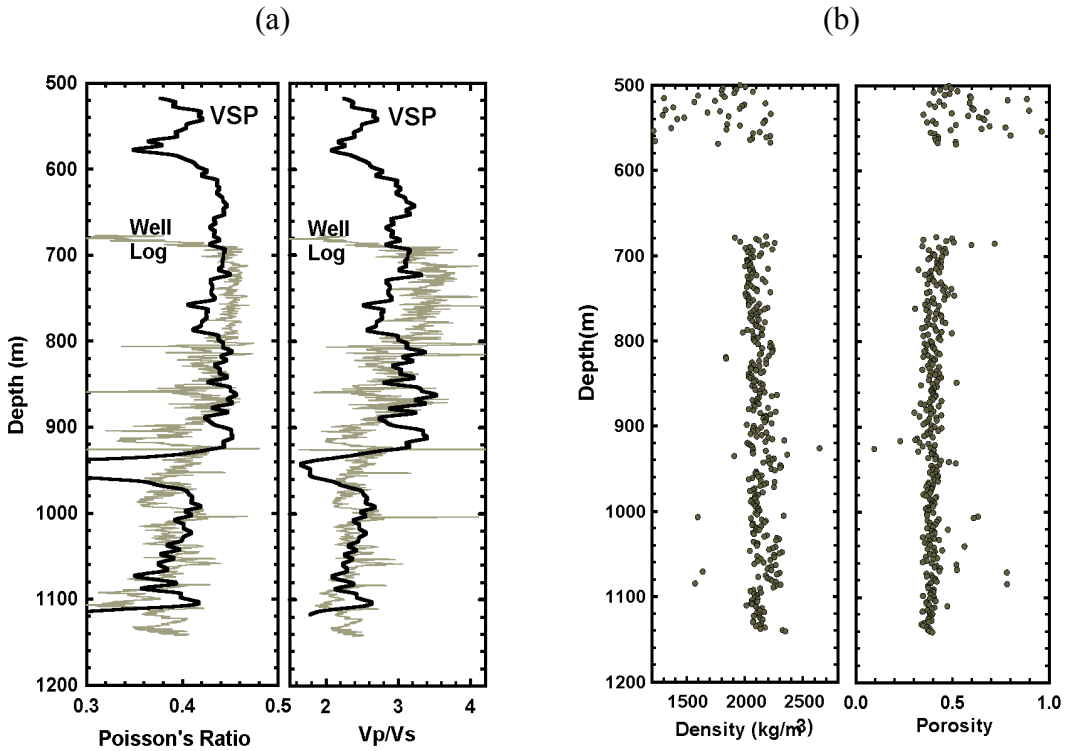

Figure 7. a) Vp/Vs and Poisson's ratio calculated from VSP and sonic velocities, b) density and porosity derived from well log.

A small amount of free gas (less than 5%) can cause a dramatic P-wave velocity decrease and a low Poisson's ratio is expected within free-gas bearing sediments (Yuan et al., 1996, 1999). For marine unconsolidated sediment, the first 5% of free gas below the gas hydrate stability zone causes the Poisson's ratio to drop from 0.48 to 0.42. An abnormally low P-wave velocity zone was evidenced in the DSI log processing procedure. The low velocity zone the occur after the first two gas hydrate layers roughly follow the background velocity profile, while P-wave velocity below the third gas hydrate layers is excessively low, leading to a low Vp/Vs ratio of 1.9 and a low Poisson's ratio of 0.31.

ESTIMATE GAS HYDRATE SATURATION

The most readily observable change in the physical properties of sediment , resulting from the presence of gas hydrate, is the increase in seismic velocity. The acoustic velocity of pure gas hydrate is about 3700 m/s (Pearson et al, 1983; Sloan, 1990). Cemented by gas hydrate, the P velocity of normal sediments can vary from 2700 m/s to 6000 m/s, depending on the lithology, the type of gas hydrate and its saturation (e.g., Stoll et al., 1971; Stoll, 1974; Pearson et al., 1986). Taken away with temperature estimation, increased seismic velocity is a direct indicator of the presence of gas hydrate.

In Wyllie's time-average equation (Wyllie et al, 1958), the rock slowness is taken as the weighted sum of the various constituents. The three-phase time-average equation has been applied to rocks in permafrost zones by Timur (Timur 1968) and to gas hydrate bearing rocks by Pearson et al (1983). This equation qualitatively

explains the high P-wave velocity in hydrate-bearing rocks. Lee et al (1996) discuss several models for P-wave velocity estimation for marine hydrate-bearing sediments, which are mostly unconsolidated, and concluded that the weighted three-phase time-average equation with appropriate weighting factor and lithification simulating factor is appropriate for marine sediment. The extreme case of this equation approaches the time-average equation when the sediments are a totally consolidated matrix. Similar studies by Desmons (1996) and Yaun et al. (1996) also showed that gas hydrate saturation can be calculated, provided a correct reference velocity profile.

The following two methods are used in gas hydrate saturation estimation 1) weighted equation method and 2) porosity reduction method.

I. Hydrate saturation estimation by weighted equation

The major gas hydrate bearing layers in Mallik 2L-38 are semi-consolidated, matrix-supported gravel and well sorted fine and medium sandstone, with an average porosity of 40% and density of 2.10 g/cm^3 (figure 7b**)**. It is not appropriate to use either Wyllie's time average equation or Wood's equation alone, as they describe two extreme sediment types, the consolidated rocks and unconsolidated sediment. The three-phase weighted equation (Lee and Dallimore, 1996) is used to predict the relationship between the gas hydrate concentration and the P-wave velocity for sediment with certain porosity. The equation can be written as,

$$\frac{1}{V_p} = \frac{W\Phi(1-S)^n}{V_{p1}} + \frac{1-W\Phi(1-S)^n}{V_{p2}}, \tag{1}$$

where V_{p1} is the P-wave velocity derived from the three phase Wood's equation, V_{p2} is the P-wave velocity derived from Wyllie's time-average equation, W is the weighting factor,n is the constant simulating the rate of lithification with hydrate concentrations. W<1 favors time-average velocity while W>1 favors Wood's velocity. In the case of the hydrate-bearing semi-consolidated sediment, a weighting factor favoring the three-phase time-average Wyllie's equation is expected.

Wood's three-phase time-average equation can be written as

$$\frac{1}{\rho V^2_{p1}} = \frac{\Phi(1-S)}{\rho_w V_w^2} + \frac{\Phi S}{\rho_h V_h^2} + \frac{(1-\Phi)}{\rho_m V_m^2}, \tag{2}$$

and the three-phase Wyllie's equation can be written as

$$\frac{1}{V_{p2}} = \frac{\Phi(1-S)}{V_w} + \frac{\Phi S}{V_h} + \frac{(1-\Phi)}{V_m}, \tag{3}$$

where V_p is P-wave velocity of the hydrated sediment, V_h is P-wave velocity of the pure gas hydrate, V_w is P-wave velocity of the pore fluid, V_m is P-wave velocity of the rock matrix, Φ is porosity as a fraction of total volume, S is gas hydrate concentration as a fraction of the pore space.

For hydrate-free sediment, the matrix density, or particle density of sediment can be calculated using

$$\rho_m = \frac{\rho - \rho_w \Phi}{(1.0 - \Phi)}, \tag{4}$$

while for hydrate-bearing sediment, it can be calculated using:

$$\rho_m = \frac{\rho - \rho_h \Phi S - \rho_w \Phi (1 - S)}{(1.0 - \Phi)}. \tag{5}$$

Lee and Collet (1999) use the same theory to estimate gas hydrate saturation based on sonic log data. The weighting factor is determined from the porosity-Vp relationship determined from the non-hydrated sediment between 748 m and 897 m in a least-square sense. The solid curves in figure 8a show hydrate saturation predicted from sonic velocity using a weighting factor of 1.56 for typical porosity values from 0.34 to 0.46. For the hydrate free sediment at approximately 678 m, with an average porosity of 0.42 and an average Vp of 1900 m/s , the equation with W=1.56 predict Vp=1750 m/s, which is about 150 m/s lower than the well log and the VSP velocities. For normal sediment immediately above the gas hydrate zone (890 m) with an average porosity of 0.36, this equation predicts a Vp of 2000 m/s, which is about 200-300 m/s lower.A different approach is taken in estimation of the weighting factor. Using the density, porosity and velocities from the hydrate-free sediment, we determined the exact weighting factor for each data sample by setting the hydrate consaturation in equation (1) to zero and then determining the optimum weighting factor by examining its distribution pattern. The distribution of the factor is found to be rather Gaussian, with a peak occuring at w=0.7385 and a standard deviation of 0.3345. Rarely is there any value larger than 1.40 to be found(figure 8b).

The density difference between pore fluid and gas hydrate is rather small and the error caused in hydrate saturation calculation is negligible according to Lee and Collet (1999). In their study, the porosity error is no more than 2% for a high hydrate concentration of 80% of pore space. This error is even smaller for low concentration cases. Rather than using equation (5), equation (4) is used to approximate the relationship between density and porosity.

Another factor to be considered in the calculation is the matrix velocity, which affects the reference velocity scheme. Normally a low reference velocity scheme leads to higher hydrate saturation values. However, since pore fluid and hydrate saturation form a more dominant factor in sediment velocity prediction, the error caused by minor errors in the matrix velocity should be small. The matrix P and S-wave velocities of sandstones with porosity from 0.02 to 0.3 and various clay content levels, were examined by Han et al (1986). Matrix velocity can be predicted by using appropriate velocity – porosity relationships. Lee and Collet (1999) predict a matrix velocity of 5.37 km/s. This value seems too high for the following reasons: 1) the velocity-porosity-clay content relationship by Han et al. was derived from samples with much lower porosity than the hydrate host sediment; 2) the experiment confining pressure (40 Mpa) is much higher than the in-situ pressure in the gas hydrate zone (20 Mpa); 3) the experiment samples are well-consolidated sandstone, not semi-consolidated hydrate host sediments.

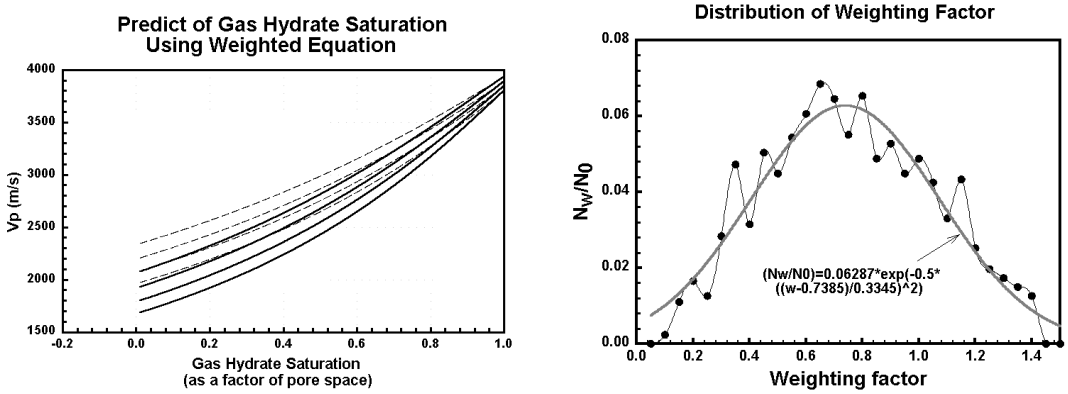

(a) (b)

Figure 8. a) Predicted Vp of hydrate host sediment using weighting factors of 0.738 (dashed lines) and 1.56 by Lee, 1996 (solid lines). From top to bottom, the sediment porosities are 34%, 38%, 42% and 46 %; b) Weighting distribution for the hydrate free sediment. Equation (1) is modified by setting S=0.

The gas hydrate saturation is calculated using velocities from P-wave VSP and well log. Figure 9 shows the gas hydrate saturation using the parameters listed in Table 3.

Table 3. Physical parameters used in gas hydrate saturation estimation.

Parameters	Value/Calcualtion Formula	Source
Bulk density	Density log	
Matrix Density	Approximated by equation (4)	
Pore Fluid Density	1024 kg/m^3.	
Gas Hydrate Density	910 kg/m^3.	Sloan, 1998.
Vp of Hydrate host sediment	VSP velocity analysis or sonic log.	
Vp of pore fluid	1500 m/s	Lee et al. 1996
Vp of pure gas hydrate	3300 m/s	Sloan, 1998
Vp of matrix	4370 m/s.	Lee et al, 1996.
Porosity	Density-porosity.	Derived from density log.
Weighting factor	0.738	This study.
Lithification factor	1.0	Lee et al. (1996)

II. Hydrate saturation estimation by porosity reduction method.

The porosity reduction method assumes that the effects of hydrate displacing pore water may be approximated by effective porosity reduction. This method is discussed

by Yuan, 1996 and Yuan et al, 1996. A brief introduction to this method is given below.

The velocity of the hydrate-free sediment, V_{sed}, is taken from the normal sediment interval ranging from 670m to 890 m. The velocity of fully hydrate-saturated sediment, V_{hysed}, is then determined using a two-phase time-average equation (Wyllie et al., 1958),

$$\frac{1}{V_{hysed}} = \frac{\Phi}{V_{hyd}} + \frac{1-\Phi}{V_m} , \tag{6}$$

where V_{hyd}, the velocity for pure methane hydrate, is 3730 m/s (Pearson et al., 1983; Sloan, 1990) and V_m, the matrix velocity, is 4370 m/s (Lee et al,1996). When V_{hysed} and the reference hydrate-free sediment velocity available, the hydrate saturation can be estimated as being the effective porosity difference between the normal sediment and the hydrated sediment. The effective porosity of hydrate bearing sediment can be written as

$$\frac{1}{V_{sed}} = \frac{\Phi'}{V_w} + \frac{1-\Phi'}{V_{hysed}} , \tag{7}$$

where Φ' is the effective porosity of hydrate-bearing sediments. Hydrate saturation can then be calculated by $S=(\Phi-\Phi')/\Phi$.

The key in this method is to choose a reliable reference hydrate-free velocity-porosity profile. Such a velocity-porosity profile may be derived from VSP or MCS velocity analysis, as typically used in the marine case (Yuan et al, 1996, Yuan et al, 1999, Fink and Spence, 1995). For a particular lithology, velocity changes depend primarily on porosity differences. Hyndman et al. (1993b) propose a porosity-Vp profile for normal compaction process:

$$\Phi = -1.18 + \frac{8.607}{V_p} - \frac{17.89}{V_p^2} + \frac{13.94}{V_p^3} , \tag{8}$$

where Vp is in km/s. However, this porosity-velocity profile does not fit the well log data at Mallik 2L-38 very well. A locally calibrated reference porosity-Vp relation using the well log is derived in a least-square sense:

$$\Phi = -1.18 + \frac{11.5}{V_p} - \frac{28.17}{V_p^2} + \frac{23.23}{V_p^3} \tag{9}$$

Equation (9) gives minor porosity change when the velocity is greater than 2000 m/s, indicating either inappropriate density-porosity conversion or little porosity reduction due to normal compact. In a more general sense, equation (8) is employed for velocity reference.

Figure 9 shows the hydrate saturation as calculated from the two methods discussed above, using the VSP velocities. Both of the reference velocity schemes of equation (8) and (9) are used in the porosity reduction method. The estimation

achieved using sonic log velocity is also shown for comparison. Hydrate saturation estimated from VSP and sonic velocities are highly correlated using the same method, while differ for different methods. A weighted equation generally gives higher values than that calculated from porosity reduction methods. However, the difference between them appears to increase with hydrate saturation.

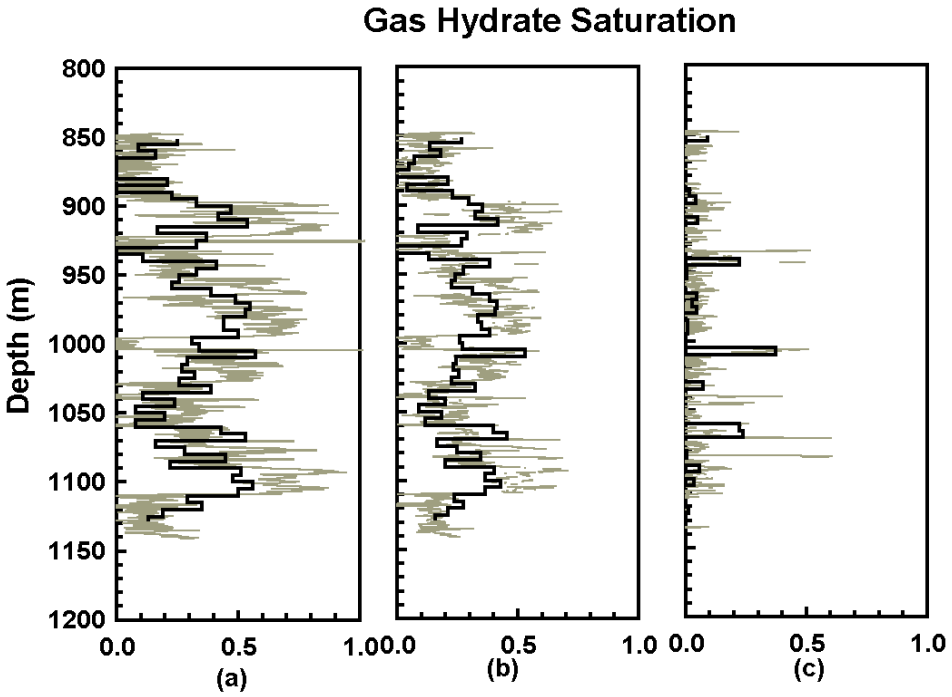

Figure 9. Gas hydrate saturation from 847 m to the bottom of the well. (a) using weighted equation with W=0.74 and n=1; (b) porosity reduction using the reference velocity scheme by Hyndman et al.,1993b; and (c) porosity reduction using the reference velocity scheme derived from the well log.

SEISMIC QUALITY FACTOR ANALYSIS

Seismic quality factor describes the anelastic attenuation of a propagating wave due to internal friction in materials and is recognized as a significant seismic parameter that improves the lithology identification, the quality of forward modeling, seismic resolution enhancement by inverse Q filter, as well as amplitude versus offset (AVO) analysis. Gas hydrate effectively reduces the internal friction by cementing the sediment particles and replacing the pore fluid, thereby reducing energy loss within the gas hydrate host sediment.

The most accurate method for Q estimation is the amplitude ratio method, which is suitable for effective Q estimation using surface seismic data, check shot or VSP data (Bath, 1974). This method provide fairly reliable Q estimation compared to other methods, such as spectral modeling (SM) (Bath, 1974, Babbel, 1984) and the analytical signal method (ASM) (Engelhard et al, 1986; Engelhard, 1990). For VSP

data down-going wavefield, the Q value is related to the amplitude ratio at depth levels 1 and 2 by:

$$\ln[\frac{|A(\omega)_2|}{|A(\omega)_1|}] = \ln[\frac{|A_{20}|}{|A_{10}|}] + \frac{(t_2 - t_1)}{2Q}\omega \quad , \tag{10}$$

where $A(\omega)_1$ and $A(\omega)_2$ are amplitude spectra at depth levels 1 (shallower) and 2 (deeper), A_{10} and A_{20} are the maximum amplitude value occurred in $A(\omega)_1$ and $A(\omega)$ and t_2 and t_1 are down-going wavefield travel time. The Q value can be calculated from the slope of the power ratio (dB/Hz) with:

$$Q = 27.3\frac{\Delta t}{S} \quad , \tag{11}$$

where Δt is the travel time difference and S is the slope of the power ratio (dB/Hz).

Frequency dependent attenuation is clearly observed in the zero-offset vertical component data (P-wave). Figure 10a shows the power spectrum of the down-going wavefield at depth levels 590 m and 835 m within the normal sediment section and 890 m and 1135 m within the hydrate host sediment. The dominant bandwidth ranges from 30 Hz o120 Hz, but signal also exists beyond 120 Hz up to 200 Hz (30 dB down) within the normal sediment and up to 180 Hz (30 dB down) in the hydrate host sediments.

The attenuation effect within the normal sediment column appears to be relatively frequency dependent. For a dominant bandwidth ranging from 50-100 Hz, a Q of 30 fits quite well. For a higher frequency, over 100 Hz, a slightly higher Q of 73 gives a rather reasonable fit.

Destructive interbed multiple interference always presents a tough condition for reliable Q analysis. For the normal sediment, this effect should be rather Gaussian and should not give much change in the spectral ratio trend because there was no major reflector within this zone to cause severe destruction at a certain frequency. Obviously, this effect prevents reliable Q estimation in the gas hydrate host sediment. The sonic log data and VSP velocity analysis both unambiguously show that there are three high velocity layers within the hydrate zone. Interbed multiples cause a notch at 50 Hz and the overall spectral variation within the dominant bandwidth is smeared. However, since gas hydrate stiffens the sediment, a Q value higher than that of normal sediment is expected.

DISCUSSION, CONCLUSIONS AND FUTURE WORK

Velocities derived from both the VSP and sonic log data unambiguously indicate the presence of high velocity zones between 890 m and 1145 m in the Mallik 2L-38 well. These high velocities are indirect indicators of the presence of gas hydrate, as massive hydrate samples were recovered from these high velocity zones. Offset VSP-CDP transform gave a P section in the vicinity of the well and suggest that the spatial hydrate distribution is fairly horizontal and that lithology must be a major controling factor in its formation. The recovered drilling cores suggest high gas hydrate

saturation in the pore space, which raises the difficulties in various hydrate saturation estimation methods, which are based on certain physical models. Weighted equation gives a rather high hydrate saturation up to 85-90% of pore space within the high velocity zones. This is consistent with the estimation from well log resistivity and weighted equation using different weighting factor and matrix velocities. It seems that changing the weighting factor from 0.74 (this paper) to 1.56 (Lee et al, 1999) and the matrix velocity from 4370 m/s to 5370 m/s (Lee et al, 1999) does not cause much difference in the hydrate saturation. Porosity reduction method based on an empirical porosity-Vp relationship derived from various deposition environments, gives a slightly lower estimation. The maximum saturation is around 60 %. The locally calibrated porosity-Vp relationship does not seem to be good since the increase of Vp does not require normal porosity reduction.

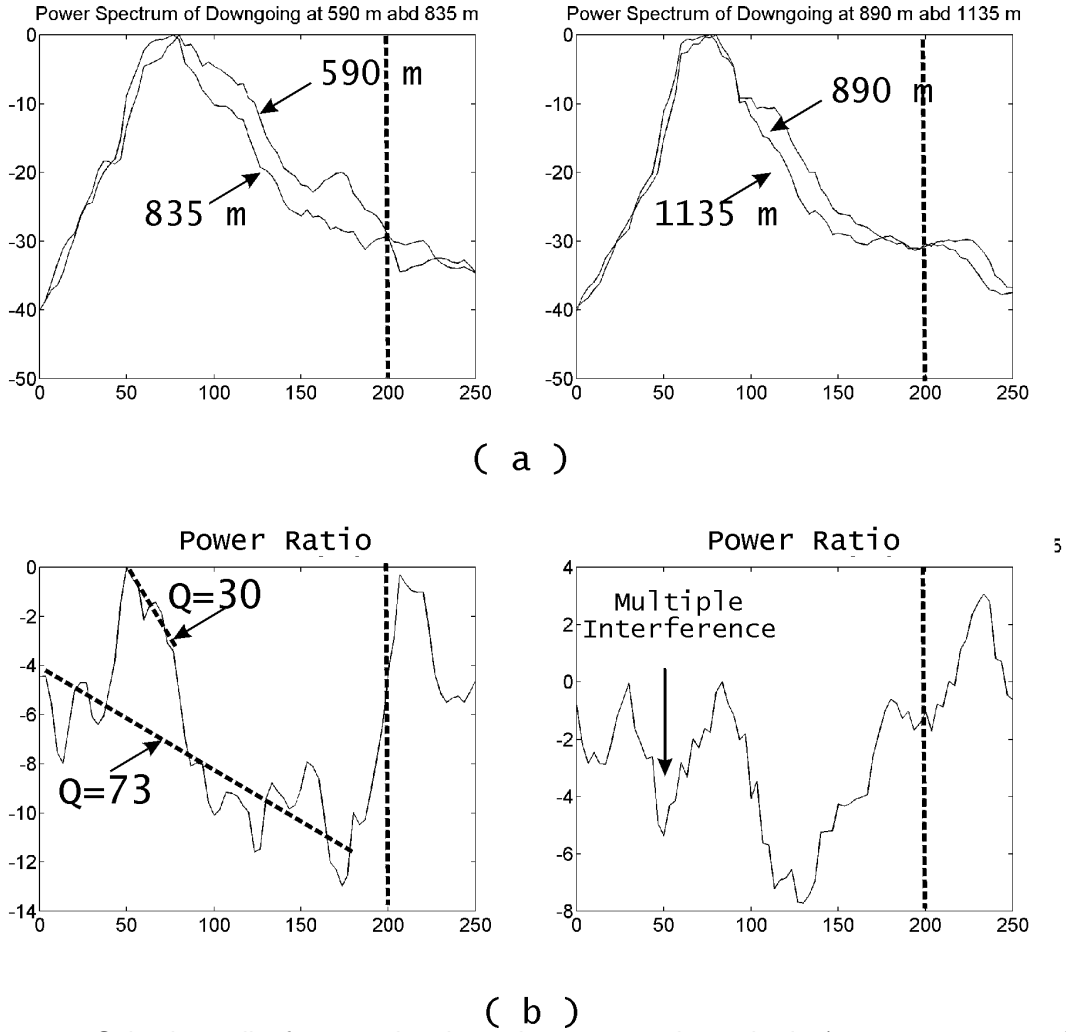

Figure 10. Seismic quality factor estimation using power ratio method, a) power spectrum of down-going wavefield at 590 m and 835 m (left) within the normal sediment section and at 890 m and 1135 m (right) within the hydrate host sediment; b) Power ratios calculated from a). Destructive multiple interference cause a notch at 50 Hz in the hydrate host sediment.

The spectral ratio method for Q estimation has been considered a rather accurate method (Tonn, 1991) and is not very sensitive to the selected time window length if the window is large enough. This has been demonstrated by several authors (Sams and Goldberg, 1990). Source signature variation is not serious and the receiver locations have been carefully selected and are believed to be optimal, thereby validating the assumption of constant source signature and receiver response.

Although the bandwidth of the zero-offset P-wave data extends to 200 Hz, the effective bandwidth is narrow and the signal rapidly decreases after 90 Hz, making the Q estimation for high frequency data unreliable. Multiple interference is not a serious problem in the normal sediment section, while causes serious damage to the power spectra in the hydrate host sediments. An effective Q value within the dominant frequency band (50-100 Hz) can not be obtained. However, a Q value higher than the normal sediment is expected in the hydrated sediments. The destructive interbed multiple causes at least 2.6 dB down at 50 Hz. A Q value of 30 was estimated from the dominant band for the normal sediment section. This value seems slightly low compared to the measurement done on clayey and silty sand, which has an average Q of 26 (Badri and Mooney, 1986).

Reflectivity correction can be done before calculating the spectral ratio. There is no major strong reflection within the normal sediment so that the reflectivity is rather Gaussian, so that reflectivity correction will not cause major changes in calculating the power ratio. This correction is obviously necessary in the hydrate zone, where reflectivity becomes non-Gaussian. This will be carried out in future research.

ACKNOWLEDGEMENT

This paper would not have been possible without the support and advices offered by Dr. Hyndman and Dr. Dallimore of Geological Survey of Canada, Dr. Rakesh Walia of CGG Canada, and Dr. Sakai of Japan National Oil Cooperation (JNOC). Dr. Lee of USGS provided well processed well log data, which made the integration of the seismic and well log data possible. We would also like to extend my thanks to Dr. Margrave of the CREWES Project for many important suggestions and the steering committee for the Mallik gas hydrate research project for the excellent data acquisition. Finally, we would like to extend our thanks to the CREWES sponsors.

REFERENCES

Andreassen, K., P.E. Hart and A. Grantz,1995, Seismic studies of a bottom simulating reflection related to gas hydrate beneath the continental margin of Beaufort Sea, Journal of Geophysical Research, **Vol**. 100, 12659-12673.

Bath, M., 1974, Spectral analysis in geophysics, Development in Solid Earth Geophysics, M. Bath (ed.), **Vol**. 7, Elsevier Publishing Co.

Badri, M, and Mooney, H.M., 1986, Q measurements from compressional seismic waves in unconsolidated sediments, Geophysics, **Vol**. 52, 772-784.

Bily, C., and Dick, J.W.L., 1974, Natural occuring gas hydrate in the Mackenzie Delta, Northwest Territories, Bulletin of Canadian Petroleum Geology, **Vol**. 22, no. 3, p. 340-352.

Castagna, J.P., M.L. Batzle, and R.L. Eastwood, 1985, Relationships between compressional-wave and shear-wave velocities in clastic silicate rocks, Geophysics, **Vol**. 50, 571-581.

Collet, T.S. and Dallimore S.R., 1998. Quantitative assessment of gas hydrates in the Mallik L-38 Well, Mackenzie Delta, N.W.T.. Proceedings of the 7th International Conference on Permafrost, Yellowknife, Canada, June 1998.

Dallimore S.R., and Collet, T.S., 1995. Intrapermafrost gas hydrates from a deep core hole in the Mackenzie Delta, Northwest Territories, Canada, Geology, **Vol**. 23, no. 6, p. 527-530.

Dallimore, S.R., Uchida, T. and Collet, T.S., 1998, JAPEX/JNOC/GSC Mallik 2L-38 Gas hydrate research well: overview of science program, JNOC "Methane Hydrate: Resources in the near future?, ", p. 311-318, JNOC-TRC, Japan.

Desmons, B., Integrated study of gas hydrates in marine sediments using geophysical and geochemical data, M.S. Thesis, University of Victoria, Victoria, B.C., 1996.

Dixon, J., Dietrich, J.R. and McNeil, D.H., 1992, Upper Cretaceous to Pleistocence sequence stratigraphy of the Beaufort – Mackenzie and Banks Island areas, northwest Canada, GSC Bulletin, 407, 90 p.

Engelhard, L., Doan, D., Dohr, G., Drewes, P., Gross, T., Neupert, F., Sattlegger, J. and Schonfeld, U., 1986, Determination of the attenuation of seismic waves from actual field data, as well as considerations to fundamental questions from model and laboratory measurements, DGMK Report 254, 83-119.

Hardage, B.A., Toksöz, M. N. and Stewart, R. R. 1983-1984, Vertical seismic profiling (2nd ed), Geophysical Press, London.

Han, D-H, Nur, A., and Morgan, D., 1986, Effects of porosity and clay content on wave velocities in sandstones, Geophysics, **Vol**. 51, NO. 11, 2093-2107

Hyndman, R.D., and Spence, G.D., 1992, A seismic study of methane hydrate marine bottom simulating reflectors by vertical fluid expulsion, Journal of Geophysical Research, **Vol**. 97, 6683-6698.

Hyndman, R.D., G.F., Moore, and K. Morgan, Velocity porosity and pore-fluid loss from the Nankai subduction zone accretionary prism, edited by I.A. Hill, et al, Proceeding of Ocean Drilling Program, Scientific Results, 131, 211-220, 1993.

Jenner, K. A., Dallimore, S. R., Nixon, F. M., Winters, W., and Uchida, T., Sedimentology of methane hydrate host strata from JAPEX/JNOC/GSC Mallik 2L-38, JNOC "Methane Hydrate: Resources in the near future?, ", p. 319-326, JNOC-TRC, Japan.

Judge, A.S., Pelletier, B.R., and Norquay, I., 1988. Permafrost base and distribution of gas hydrates, in Marine Science Atlas of the Beaufort Sea. (Pelletier, B.R.. Ed.). Geological Survey of Canada, Miscellaneous Report 40.

Lee, M.W., Hutchinson, D.R., Collet, T.S., and Dillon, W.P., 1996, Seismic velocities for hydrate-bearing sediments using weighted equation, Journal of Geophysical Research, **Vol**. 101, 20,347-20,358.

Lee M.W. and Collet, T.S., 1999, Amount of gas hydrate estimated from compressional- and shear-wave velocities at the JAPEX/JNOC/GSC 2L-38 gas hydrate research well, GSC Bulletin 544, 313-322.

Pandit, B.I. and M.S. King, 1983, Elastic wave velocities of propane gas hydrates, in Natural Gas Hydrate: Properties, Occurrence and Recovery, edited by J.L. Cox, 49-61, Butterworth, Stoneham, Mass.

Pearson, C.F., P.M.. Halleck, P.L. McGuire, R. Hermes, and M. Mathews, 1983, Natural gas hydrate: A review of in situ properties, J. Phys. Chem., **Vol**. 87, 4180-4185.

Pearson, C.F., J. Murphy, and R. Hermes, 1986,Acoustic and resistivity measurements on rock samples containing hydrates: Laboratory analogues to natural gas hydrate deposits, Journal of Geophysical Research, **Vol**, 91, 14,132-14,138.

Raikes, S.A., and White, R.E., 1984, measurements of Earth attenuation from downhole and surface seismic recordings, Geophysical Prospecting, **Vol**. 32, 892-919.

Sakai, A., 1998, Vertical seismic survey in the Mallik 2L-38-specifications, data acquisitions and data analysis, JNOC "Methane Hydrate: Resources in the near future?, ", p. 358-370, JNOC-TRC, Japan.

Sakai, A., 1999, Velocity analysis of vertical seismic profile (VSP) survey at JAPEX /JNOC/GSC Mallik 2L-38 gas hydrate research well, and related problems for estimating gas hydrate concentration, GSC Bulletin 544, 323-340.

Sams, M. and Goldberg, D., 1990, The validity of Q estimates from borehole data using spectral ratios, Geophysics, **Vol**. 55, 97-101.

Sloan, E.D., 1990, Clathrate hydrates of natural gases, 641 pp., Marcel Dekker, New York.

Sloan, E.D., 1998, Clathrate hydrates of natural gases, Marcel Dekker, New York.

Stoll, R.D., J. Ewing, and G.M. Bryan, 1971, Anomalous wave velocities in sediments containing gas hydrate, Journal of Geophysical Research, **Vol**.76, 2090-2094, 1971.

Stoll, R.D. 1974, Effects of gas hydrates in sediments, in Natural Gases in Marine Sediments, edited by I.R. Kaplan, pp. 235-248, Plenum , New York.

Timur, A., 1968, Velocity of compressional waves in porous media at permafrost temperatures, Geophysics, **Vol**. 33, 584-595.

Tonn, R., 1991, The determination of the seismic quality factor Q from VSP data: A comparison of different computational methods, Geophysical Prospecting, **Vol**.39, 1-27.

Walia, R., Y. Mi, R.D. Hyndman, and A. Sakai, 1999, Vertical seismic profile (VSP) in the JAPEX/JNOC/GSC Mallik 2L-38 gas hydrate research well, GSC Bulletin 544, 341-356

Whalley, E., 1980, Speed of longitude sound in clathrate hydrates, Journal of Geophysical Research, **Vol**. 85, 2539-2542.

Yuan, T., Hyndman, R.D., Spence, G.D. and Desmons, B., 1996, Seismic velocity increase and deep-sea gas hydrate concentration above a bottom-simulating reflector on the northern Cascadia continental slope, Journal of Geophysical Research, **Vol**. 101, No. B6, 13655-13671

Yuan T., Spence, G.D. and Hyndman R.D., 1999, Seismic velocity studies of a gas hydrate bottom-simulating reflector on the northern Cascadia continental margin: Amplitude modeling and full waveform inversion, Journal of Geophysical Research, **Vol**. 104, NO. B1, 1179-1191.

Wyllie, M.R.J., A.R. Gregory, and G.H.F. Gardner, An experimental investigation of gactors affecting elastic wave velocities in porous media, Geophysics, **Vol**. 23, 459-493.